Polymer 55 (2014) 6418–6425

Contents lists available at ScienceDirect

Polymer

journal homepage: www.elsevier.com/locate/polymer

3-D computational model of poly (lactic acid)/halloysite nanocomposites: Predicting elastic properties and stress analysis

R.T. De Silva [a], Pooria Pasbakhsh [a, *], K.L. Goh [b], Leon Mishnaevsky Jr. [c]

[a] Multidisciplinary Platform of Advance Engineering, Mechanical Engineering Discipline, School of Engineering, Monash University Malaysia, 47500 Selangor, Malaysia
[b] School of Mechanical and Systems Engineering, Newcastle University, UK
[c] Department of Wind Energy, Technical University of Denmark, Denmark

ARTICLE INFO

Article history:
Received 19 June 2014
Received in revised form
23 September 2014
Accepted 23 September 2014
Available online 8 October 2014

Keywords:
Poly (lactic acid) (PLA)
Halloysite nanotubes (HNTs)
Finite element analysis (FEA)

ABSTRACT

A real-structure based 3-D micromechanical computational model of poly (lactic acid) nanocomposites reinforced by randomly oriented halloysite nanotubes (HNTs) was developed and compared with an idealized model (conventional model) and experimental results. The developed idealized model consists of nanotubes with fixed aspect ratio and the proposed alternative real-structure based model takes the experimentally observed variations of HNTs sizes, impurities and aspect ratios into account. The requirements of the 3-D HNTs nanocomposite models have been explored by testing idealized, real structure based models, as well as models with hollow and solid cylinder-like reinforcements with varied amounts of HNTs. A unit cell model with cylindrical reinforcements (representing HNTs) and at least 30 inclusions gave promising results, provided the model includes actual information about HNT's size ranges and aspect ratios. Numerical studies were validated with experimental investigations and the developed real-structure based model gave more accurate results than idealized and analytical models.
© 2014 Elsevier Ltd. All rights reserved.

1. Introduction

Polymer nanocomposites (PNCs), formed by incorporating small amounts of nano-scaled fillers into the polymeric matrices, demonstrate significantly enhanced physical and chemical properties. While the most widely considered nanoscale reinforcements are with carbon nanotubes (CNTs), graphene and layered nanoclays, a growing interest in the scientific community is attracted now to other, alternative nanoscale reinforcements, one of which is with halloysite nanotubes (HNTs). HNTs are natural, hollow and tubular shaped aluminosilicates with an external diameter of 20–200 nm, internal diameter of 17–50 nm, and length of 100–5000 nm [1]. HNTs have improved the elastic modulus of polyamide, epoxy and chitosan composites by 31, 22 and 21% at their optimum concentration, respectively [2–4]. These improvements are due to the nanoreinforcement effect of well dispersed HNTs and the matrix-HNTs interfacial interactions facilitated by the hydroxyl and siloxane groups originating from the edges/defect walls and surface of nanotubes, respectively.

A number of theoretical and numerical models have been developed to link the microscale structures and mechanical properties of composites [5,6]. Gómez-del Río et al. [7] demonstrated that the elastic modulus of composites (E_c) predicted by Mori–Tanaka (M–T), Halpin–Tsai (H–T) and Cox models correspond well to the experimental results obtained on poly (ethylene terephthalate)/CNTs nanocomposites. Moreover, experimental results of E_c of PLA/HNTs nanocomposites have been validated with the H–T model [8].

Computational models of composites can be categorized into a unit cell approach and real micro-structure based modelling, based on finite element and other multi-step modelling methods. While 2-D FE approach has been used to evaluate E_c by many researchers [9–11], the evidence shows that its predicted properties significantly differ from 3-D FE models [12]. While the evaluation of properties of composites and nanocomposites with aligned fibres is relatively an easy task [5], the determination of mechanical properties of nanocomposites with randomly oriented, tubular shaped fillers in 3-D space is still a challenge. Dai and Mishnaevsky Jr. [13,14] and Wang et al. [15] used the Python based code to generate 3-D FE models, and to analyse the effect of nano-reinforcement shapes and distributions on the mechanical behaviour of nanoclay reinforced polymers. The evaluation of the thermo-mechanical properties using FE models of randomly oriented CNTs [16] and

* Corresponding author. Tel.: +60 3 55146211; fax: +60 55146207.
E-mail addresses: pooria.pasbakhsh@monash.edu, ppooria@gmail.com (P. Pasbakhsh).

http://dx.doi.org/10.1016/j.polymer.2014.09.057
0032-3861/© 2014 Elsevier Ltd. All rights reserved.

fibre [17] based composites have also been reported. Hine et al. [18] generated a fibre length distribution profile (polydispersed) using a Monte Carlo algorithm and developed a 3-D, randomly positioned, but aligned fibre consisting model to predict the E_c. Yet, all the listed studies do not provide experimental validation of the computational studies (as for the case of microscale whisker reinforced composites by Lee et al. [19], for instance). Table 1 gives a short overview of various 3-D models of composites reinforced with randomly oriented and tubular shaped fillers with only a few experimental validated studies.

The introduction of real experimental parameters of nanoscale structures can improve the numerical estimations of material properties. Sheidaei et al. [20] created a 3-D model of polypropylene (PP)/HNTs nanocomposite using an image processing technique by stacking a series of scanning electron microscopy (SEM) micrographs of adjoining layers obtained by slicing the composite with a focussed ion beam. A real micro-structure based 2-D model of PP/clay composites is also reported by Dong et al. [21]. While these types of real structure based models gave more precise evaluation than the idealized unit cell models, they require much larger computation resources and longer simulation times.

Thus, the formulation of computational models (which reflect real structures of nanomaterials and is easy enough to carry out serial simulations and virtual testing of structures) is an important step to the optimal design of nanocomposites. In this work, efficient and real structure-based unit cell models of HNTs based polymer nanocomposites were developed considering the variation of dimensions of HNTs and its impurities. This efficient 3-D model was compared with the idealized model (conventional modelling approach) and the FE results from both models were compared with the experimental results of PLA/HNTs nanocomposites prepared by melt compounding in order to validate the accuracy of the models.

2. Model formulation

2.1. Idealized unit cell model of randomly oriented HNTs

A number of unit cell models with randomly distributed HNTs were generated. FE modelling was carried out with COMSOL Multiphysics (v 4.3), Structural Mechanics Module (static linear module) together with the "Live Link" extension to MATLAB. HNTs were modelled as cylinders with the length of 300 nm (based on the most frequently observed HNTs, see Fig. 1) and the aspect ratio of 12 [1]. In the cell, the central positions (x, y and z) and Euler angles of the nanotubes (θ and ϕ) were randomly generated with "live link" extension to MATLAB in COMSOL. Overlapping of nanotubes within the RVE space was avoided by assigning a minimum gap in-between themselves (the minimum gap was greater than the minimum mesh size for each model). To ensure a periodic structure, any parts of the nanotubes which were cut by a given face in the unit cell were placed on the opposite face with the same orientation. This was implemented with the aid of Boolean operator in COMSOL. An example of the generated idealized FE model or RVE is given in Fig. 2(a).

2.2. Input data and boundary conditions

Material properties of the matrix (PLA) and nanotubes (HNTs) are listed in Table 2. Elastic modulus of HNTs (E_H) is reported as 71–133 GPa [24] and 140 GPa (average) [25]. In this study E_H assumed at the level of 140 GPa according to the average E_H (140 GPa) reported by Lecouvet et al. [25] and following the numerical studies conducted for the same type of HNTs (Matauri Bay from Imerys) [20]. Displacement controlled symmetric boundary conditions were applied to the RVEs. The boundary conditions are as follow;

$$\begin{aligned} u(\mathrm{BCFG}) &= 0 \\ v(\mathrm{ABGH}) &= 0 \\ w(\mathrm{HGFE}) &= 0 \\ v(\mathrm{DCFE}) &= -\delta \end{aligned} \tag{1}$$

Letters A–H denote to the points as marked in Fig. 2(a) which used to represent the planes.u, v and w denote to the displacements in X, Y and Z direction, respectively. δ is the prescribed displacement applied on the plane. As described in equation (1), displacements of the planes BCFG, ABGH, HGFE was restricted in the normal direction and a prescribed displacement was applied to the plane DCFE. Prior to simulations, the nanotubes and matrix of the models were separately meshed with tetrahedral elements (Fig. 2(c) and (d)).

E_c was determined in the simulations, using the linear solver of COMSOL by assigning a prescribed displacement of 1% strain (linearity was confirmed experimentally) with a step size of 0.25% on plane DCFE. After simulating the model, stress on the strain applied area (plane DCFE) was determined and plotted against applied strains. Then the gradient of the plotted curve was

Table 1
Accuracy of predicting elastic modulus of (nano)composites reinforced by randomly oriented, tubular shaped fillers in 3D space using FE and analytical models.

Composite type	Varied factors		Methods	Difference between methods
	Aspect ratio	Amount		
polypropylene/HNT [20]	–	5 wt%	1. Experimental 2. Object oriented – FEA 3. Statistical (TPCF) – FEA	1 & 2 is 8.8% 1 & 3 is 5.7%
Alloy/whiskers [14]	–	15 v%	1. Experimental 2. FEA 3. H–T model	1 & 2 is 1.6% 1 & 3 is 6.6%
polyamide/cylindrical filler [13]	5	5 v%	1. FEA (ideal model) 2. FEA (correlated model)	1 & 2 is ≈1%
Epoxy/CNT [16]	100–1000	1–10 v%	1. FEA (3D RVE) 2. FEA (2D RVE) 3. H–T model	1 & 3 is 3.5–36.5%
Polymer/cylindrical shape filler [22]	50	3 v%	1. FEA 2. Mori–Tanaka 3. Statistical (TPCF)	1 & 2 is 9.6% 1 & 3 is 4.5%
Short fibre reinforced alloy [17]	1–15	10–40 v%	1. FEA 2. Self-consistent method	1 & 2 is ≈3%
Poly(methyl methacrylate)/CNT [23]	10–1000	Up to 0.4 v%	1. Mori–Tanaka 2. Micromechanics with interphase	–

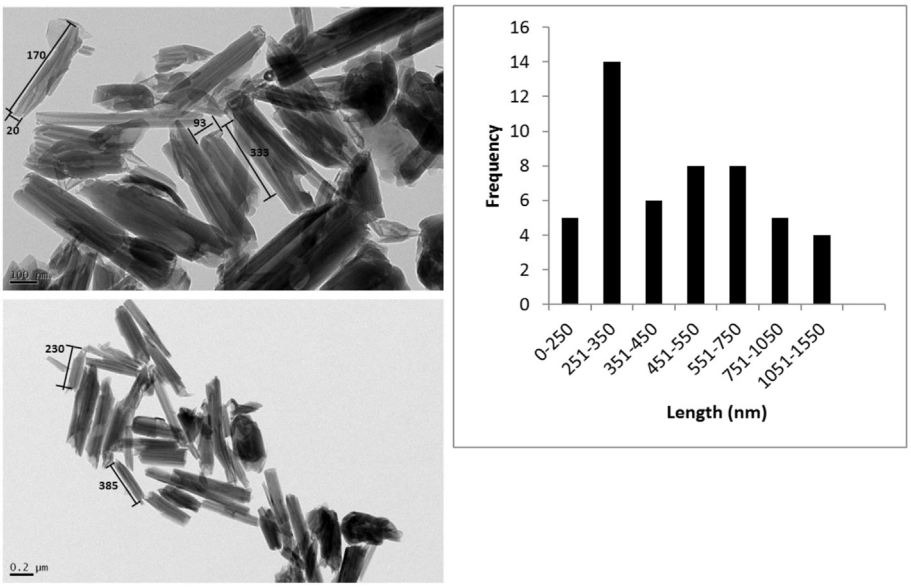

Fig. 1. Histogram of frequency versus HNT length. The data was obtained by measuring individual HNTs based on TEM images (insets).

calculated to determine the E_c. Five different models (with different random orientations of HNTs) were simulated to calculate the average E_c for each composition (2.5, 5, 7.5 and 10 (w/w %) of HNTs).

2.3. Real structure parameters based unit cell model

To improve the presented idealized model, factors such as variations of the length, diameters, range of aspect ratios and impurities of HNTs were considered to make a real structure based model. The HNTs consisted of long and thin, short and stubby, tubular, un-wrapped and spheroidal nanotubes, and some impurities [1]. Therefore, length profile details of HNTs were evaluated by taking 50 measurements of HNTs' lengths out of 30 TEM micrographs (histogram, Fig. 1), where the lengths were categorized to 7 segments from 0 to 1600 nm. The mean value of each segment was selected as the length of the cylinders for the model and the representation of the nanotubes were decided based on the frequency parameter of the histogram. 9, 25.2, 10.8, 14.4, 14.4, 9 and 7.2% of HNTs represented mean lengths of 125, 300, 400, 500, 650, 900 and 1300 nm, respectively. The level of 10% was chosen as the percentage of impurities [1]. The average diameter of each segment was also inserted as the input parameter in the model. The real structure based RVEs were modelled and simulated in a similar way to the idealized model as described in Section 2.1 and 2.2 (Fig. 2(b)).

3. Model analysis and parameter studies

3.1. Parameter studies: sensitivity to the number of nanotubes

The effect of the RVE sizes (i.e. amount of reinforcing particles) on the output of simulations was studied by testing the models with 10, 30 and 60 nanotubes (Table 3). Although the statistical analysis (one-way ANOVA) revealed that the deviations of the predicted modulus values are not statistically significant in the models with 10, 30 and 60 nanotubes ($P > 0.05$) the model with 10 tubes somewhat showed larger deviations from the results with 30 and 60 tubes (Table 3). The difference between the E_c calculated using the models with 30 and 60 tubes is 0.0019, which is rather small. Similar results were reported in the literature [12,26]. Therefore in this study, the model with 30 tubes was used to evaluate E_c, to avoid the overlong computational time.

3.2. Solid cylinder model versus hollow cylinder model

The permissibility of the representation of hollow (HC) cylinder HNTs by a solid cylinder (SC) in the simulations was evaluated. Two simple models (with only one tube/cylinder reinforcements) were developed. The length and aspect ratio of both SC and HC models were set to 300 nm and 12, respectively (see Section 3.1). The RVEs were modelled as cuboids where the length was 400 nm. The unit cell size was determined by calculating the corresponding volumes of PLA/HNTs nanocomposite, reinforced with 2.5 (w/w %) of HNTs and symmetric boundary conditions were applied. E_c for SC and HC based materials were determined to be 1.905 and 1.948 GPa, respectively, which is a 2.2% difference. Therefore, SC was selected as the simplified geometrical entity to represent HNTs in the developed multi-element 3-D models in this study. The error difference between the RVEs could be reduced when the number of nanotubes increases; the difference between SC and HC based models were reduced to 1.6% when the RVEs with 2 nanotubes each were simulated (not shown here). Moreover, it is valid to model HNTs as solid cylinders since no evacuation has been conducted (Section 4.1) to remove the air from HNTs' lumen space to promote polymer chain penetration.

3.3. Idealized model versus real structure based model

The simulated E_c of the real structure based model shows less deviation from the experimental data compared to the idealized model; especially at high HNTs concentrations (7.5 and 10 (w/w %)) (Fig. 3). For instance, at 10 (w/w %), simulated E_c values of idealized and real structure based models deviate from the experimental results by 14.97% and 10.3%, respectively. This could be mainly due to the (i) presence of a range of aspect ratios (5–12), (ii) effective reduction of 'contact surface area to RVE volume ratio' (ξ) and (iii) modelling impurities as spheres in real structure based model compared to the idealized model. When the aspect ratio of the fillers decreases, longitudinal modulus decreases [18,23,27,28]. Hence, in a real structure based model the presence of tubes with

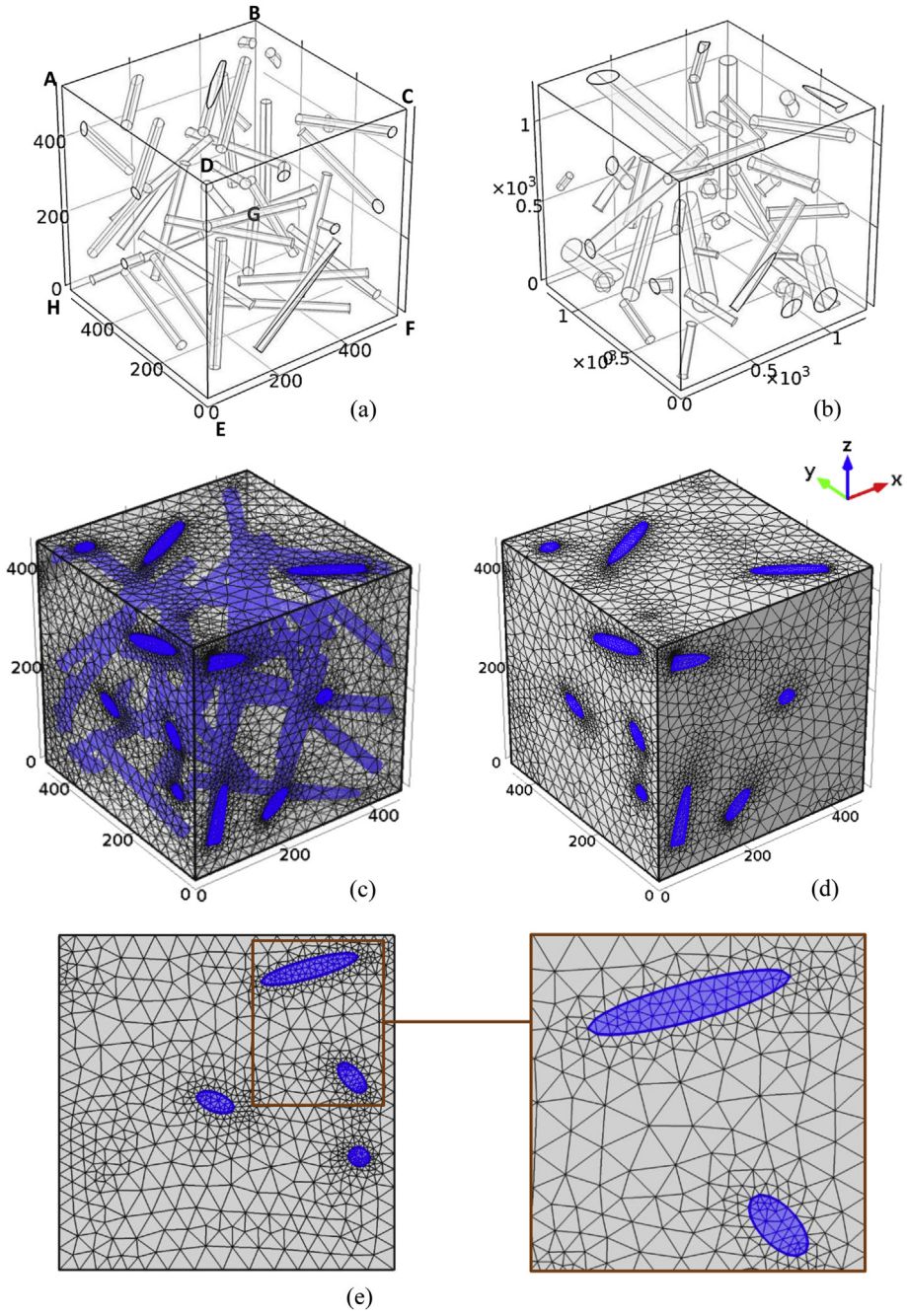

Fig. 2. RVE with randomly distributed fillers. (a) idealized, (b) real structure based models of nanocomposite with 5 (w/w %) of HNTs, (c) & (d) Meshed RVE models and (e) one of the side views of the meshed RVE.

lower aspect ratios (<12) in the axial direction could result in reduction of E_c. Moreover, a range of aspect ratios of fillers lead to effective reduction of ξ; for instance at 5 (w/w %), ξ of idealized and real structure based models are 4.3×10^{-3} nm^{-1} and 0.793×10^{-3} nm^{-1}, respectively. When ξ decreases, the efficiency of stress transfer from the matrix to fillers decreases. Furthermore, modelling the impurities as spherical elements within the RVE led to inefficient stress transfer from matrix to the impurities. The efficiency of stress transfer from matrix to spherical shaped fillers is lower than the angular particles, cylinders, disks and elliposides [15,29]. Predicted E_c values of real structure based model converge

Table 2
Assigned material properties in the simulations.

	Elastic modulus (GPa)	Density (kg/cm^3)	Poisson ratio
PLA	1.445	1250	0.35
HNT	140	2500	0.2

Table 3
Sensitivity of the number of nanotubes.

Number of nanotubes	Modulus results from FEA	Standard deviation
10	1.695 GPa	0.0958
30	1.795 GPa	0.0890
60	1.835 GPa	0.0871

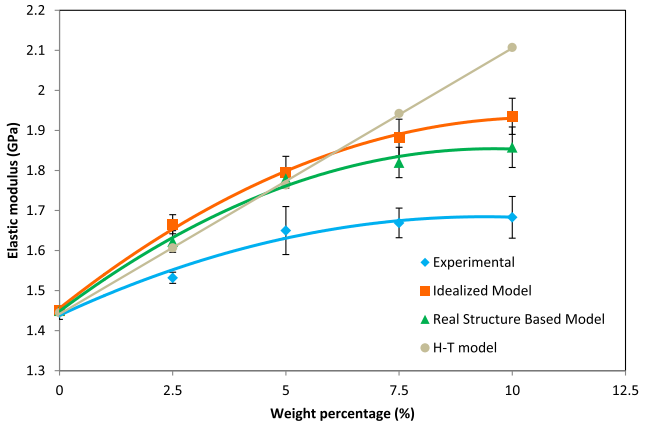

Fig. 3. Elastic modulus versus weight percentage of HNTs; (◆) experimental results, results from real structure based (▲) and idealized (■) models, and Halpin–Tsai (●) model.

towards the experimental results compared to the idealized model, but the difference between the two models is statistically insignificant for all the compositions (tested with two-way ANOVA and $P > 0.05$). The accuracy of the real structure based model can be further enhanced by (i) introducing aggregates of HNTs in to the model, (ii) modelling the interphase of nanotubes separately and (iii) increasing the average sample size (calculate E_c of each composition with at least 10 models instead of 5).

3.4. Real structure based FE model versus Halpin–Tsai model

In this section the real structure based model is compared with the modified Halpin–Tsai (H–T) model [8]. The elastic modulus of the composite according to the H–T model can be expressed as;

$$\frac{E_C}{E_m} = \frac{3}{8}E_L + \frac{5}{8}E_T \tag{2}$$

where E_L and E_T are the longitudinal and transverse modulus, respectively which can be obtained from the following equations:

$$E_L = \frac{1 + \left(\frac{2l}{d}\right) n_L V_H}{1 - n_L V_H} \tag{3}$$

$$E_T = \frac{1 + 2n_T V_H}{1 - n_T V_H} \tag{4}$$

where

$$n_L = \frac{\left(\frac{E_H}{E_m}\right) - 1}{\left(E_H/E_m + 2\frac{l}{d}\right)} \tag{5}$$

and

$$n_T = \frac{\left(\frac{E_H}{E_m}\right) - 1}{(E_H/E_m + 2)} \tag{6}$$

In the equations, E denotes to the elastic modulus and V is the volume fraction. Subscript letters H, m, L and T refer to HNT, matrix, longitudinal and transverse, respectively. l is the HNT's length and d is the HNT's diameter. To compute the H–T model, E_H, E_m and (l/d) assumed to be 140 GPa, 1.445 GPa and 12, respectively.

The results of H–T model represent a linear function, with a regression correlation value (R^2) of 0.996, while real structure based model values can be approximated by a second order polynomial (Fig. 3). FE model captures the nonlinear trend of experimental E_c well compared to the H–T model, which reflects the interference between the stress fields of HNTs as the fraction increases. At lower HNTs concentrations, E_c of the real structure based model and the H–T model do not vary appreciably, but beyond 5 (w/w %), E_c of real structure based model is well below the H–T model. The deviations could be mainly attributed to the assumption of the constant length and diameter (or fixed aspect ratio), used in the H–T model. Moreover, the contact surface areas of nanotubes are not taken into account in the H–T model. Lee et al. [19] made a similar comparison between the FE and H–T models, and reported that the H–T model has 6.6% of error compared to FE model in predicting E_c.

3.5. Stress and strain distribution

Fig. 4 shows the Von-Mises stress distribution in a surface cross section of idealized model with 5 (w/w %) HNTs. The highest stresses are localized at the nanotube's surface and the areas of high stresses extend with increasing the applied strain which shows the importance of the interface between matrix and fillers. The influence of interface on E_c has been proven in other works by modelling the interface separately [15]. Moreover, the stress concentration (in the axial direction) in the matrix is higher when tubes are close to each other (Fig. 4). The orientation of HNTs can also substantially influence the local stresses in a unidirectional tensile mode [21]. Nanotubes aligned with the applied load direction are subjected to higher stresses than other nanotubes. The stress distribution was determined for several HNTs which are aligned approximately ($\theta = 86–90^\circ$ and $\phi = 84–90^\circ$) in the direction of the applied load along the nanotube length (0–300 nm) at different applied strains (Fig. 5; stress distribution is illustrated only for one tube). The stress distribution corresponds to Cox theory, with maximum stresses in the centre and minimum at the edges of the nanotube [30]. This suggests that the micromechanical phenomenon of stress transformation from matrix to the filler, is also valid for the nano-scaled tubular inclusions. This relationship corresponds to the HNTs with different aspect ratios in the real structure based model too (not shown here).

Fig. 6 illustrates the elastic strain in the axial direction at surface cross section of idealized model with 5 (w/w %) HNTs. Shear band is initiated at the interface of nanotubes and propagates inside the matrix. As applied strain increased, the deformation (strain contours) became wider, but did not exceed the elasticity even at 1% applied strain [19]. The closely located HNTs led to higher local strain levels in the direction of applied load (Fig. 6; as circled) [11,21].

4. Experimental investigations of the deformation of PLA/HNTs nanocomposites

4.1. Fabricating PLA/HNTs nanocomposites

Prior to blending, poly (lactic acid) (PLA, grade 3051D from Nature Works Ingeo) and HNTs were dried at 50 °C for 12 h. PLA nanocomposites containing 0, 2.5, 5, 7.5 and 10 (w/w %) of HNTs were prepared by melt blending in a Brabender-internal mixer at two different rotor speeds and temperatures. Blends were first mixed for 3 min at 30 rpm and 170 °C (during the loading of HNTs), and then mixed for another 5 min at 60 rpm and 180 °C (during mixing). The batch was extracted from the mixing chamber and

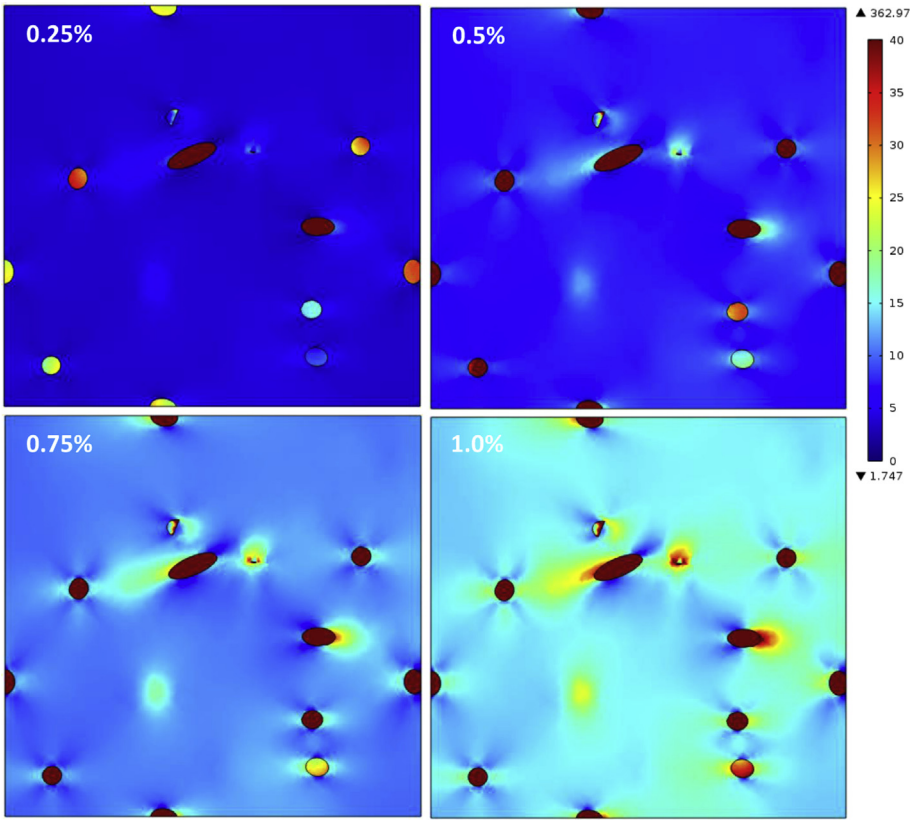

Fig. 4. Von-Mises stress distribution at surface cross section of idealized model with 5 (w/w %) HNTs at applied strains. The direction of the applied strain is horizontal to the figure. Colour codes blue to red depict the magnitudes of the stress. (For interpretation of the references to colour in this figure legend, the reader is referred to the web version of this article.)

compression moulded into films with thickness of 180–320 μm using a hot-hydraulic press at 180 °C and 5 MPa for 7 min.

4.2. Experimental results: tensile properties

Tensile properties of PLA/HNTs nanocomposites were measured using a strip tensile method based on the ASTM D882-02 standard. The nanocomposites yielded an optimum tensile strength ($\sigma = 52.5 \pm 1.7$ MPa) at 5 (w/w %), which is 22% higher than the control sample (Fig. 7). However σ decreased thereafter with addition of HNTs, but remained higher than the control sample. E_c also increased with addition of HNTs up to 5 (w/w %) and beyond that it did not increase appreciably. However, E_c improved by 16.26% with addition of 10 (w/w %) HNTs. The increment of σ and E_c could be attributed to the effective stress transfer which was facilitated by the interfacial interaction between PLA and HNTs. End

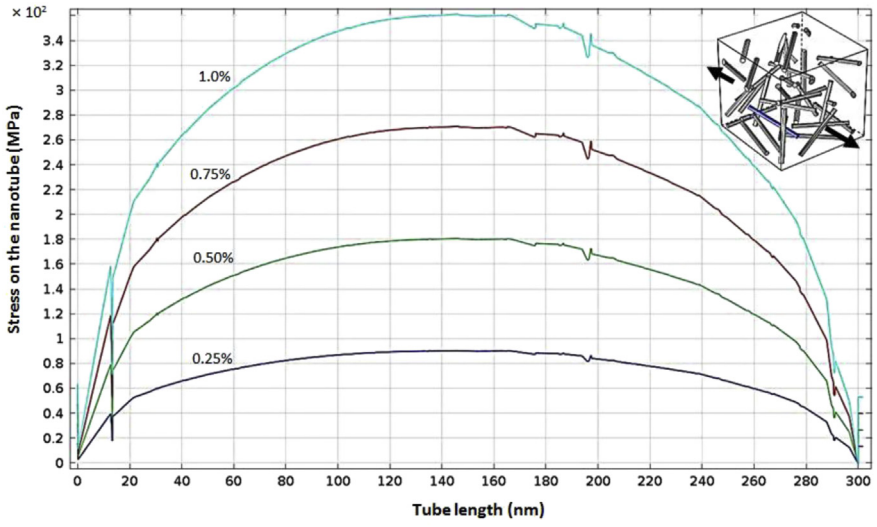

Fig. 5. Stress distribution along the length of an aligned cylinder in idealized model. The aligned cylinder is highlighted in the inset figure.

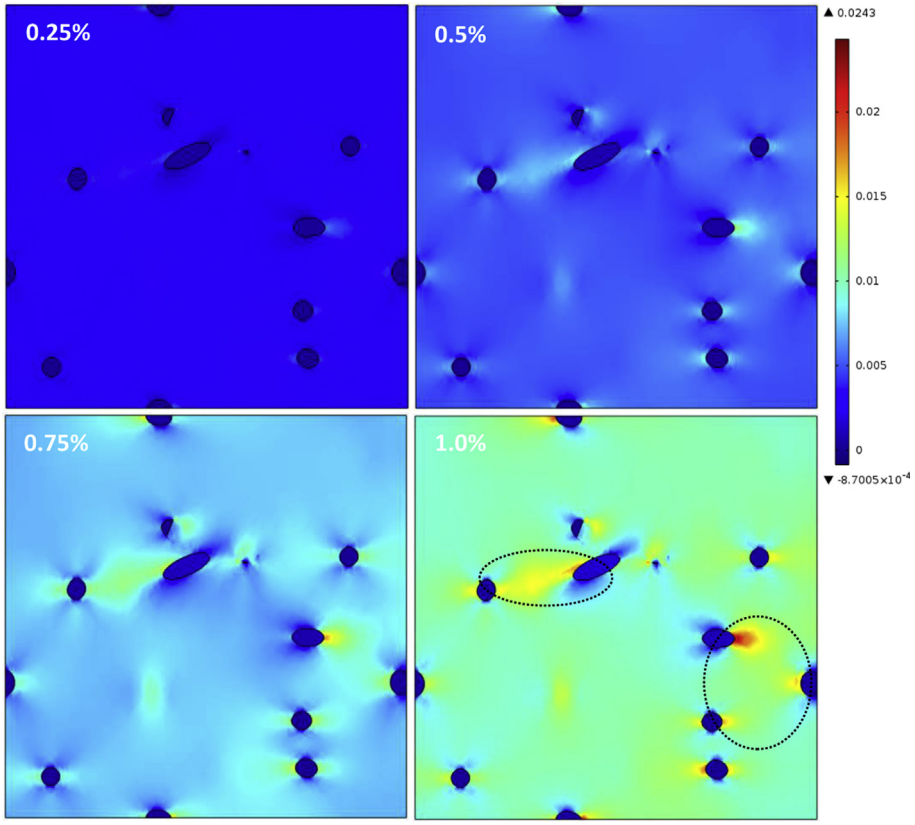

Fig. 6. Axial strain distribution at surface cross section of idealized model with 5 (w/w %) HNTs at applied strains. The direction of the applied strain is horizontal to the figure.

hydroxyl groups of PLA could possibly interact with external surface siloxane groups of HNTs via hydrogen bonding [31] or the hydroxyl groups at octahedral groups of HNTs may interact with carbonyl groups (C═O) of PLA [32]. Furthermore, the improvements of tensile properties were significant at lower HNTs concentrations due to the better dispersion of HNTs (compare micrographs; Fig. 8(a, b) versus (c, d)). Unlike σ and E_c, strain at break (ε) decreased with addition of HNTs and this could be due to the higher structural rigidity of the HNTs reinforced nanocomposites (Fig. 7).

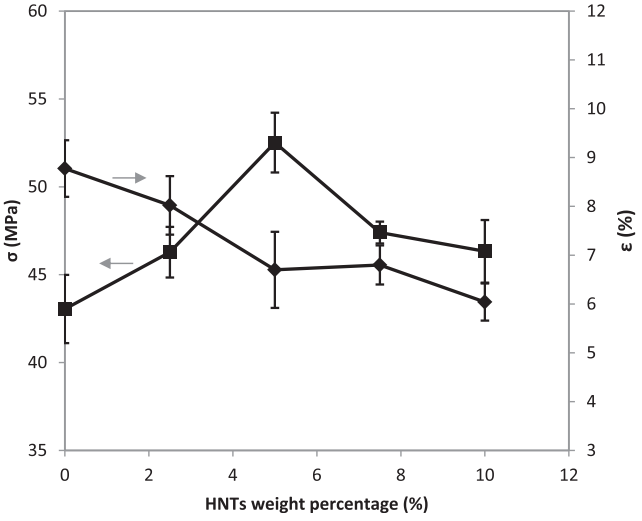

Fig. 7. Experimental results: Tensile strength (σ) (■) and strain at break (ε) (◆) versus HNTs weight concentration.

4.3. Comparison of experimental and computational results

Although FE simulations over predicted the experimentally obtained E_c, both idealized and real structure based models showed good agreement with the experimental results, especially at lower HNTs concentrations (Fig. 3). The estimations of the E_c by using idealized and real structure based model have an accuracy ranging from 8.7 to 14.98% and 5.8–10.3%, respectively (varying 2.5–10 (w/w %) HNTs). The over prediction of numerical results can be explained by the following reasons; (i) that the material properties were assumed to be isotropic, (ii) the interface between fillers and matrix is defined as perfectly bonded since meshed nodes are shared by both fillers and matrix (Fig. 2(e)) and (iii) geometrical simplification of the domains [12,19]. Therefore it can be concluded that although some complexities have been omitted in the real structure based model, this can also be used to predict E_c in a similar way to the real micro-structure based model (SEM images stacked, computer generated RVEs). Contrary to the findings of Kari et al. [17], it has been demonstrated here, that the aspect ratios of HNTs have a strong influence on the E_c, since the real structure based model (which consist of range of aspect ratios) predicted E_c more accurately than the idealized model.

5. Conclusion

A finite element (FE) based computational study was carried out to predict the elastic modulus of PLA/HNTs nanocomposites and the results were validated with experimental studies. The accuracy of an idealized 3-D model with fixed aspect ratio and randomly oriented HNTs was evaluated against an effective real structure-based model, taking into account experimentally observed variations of HNTs sizes, aspect ratios and impurities. It was found that the real

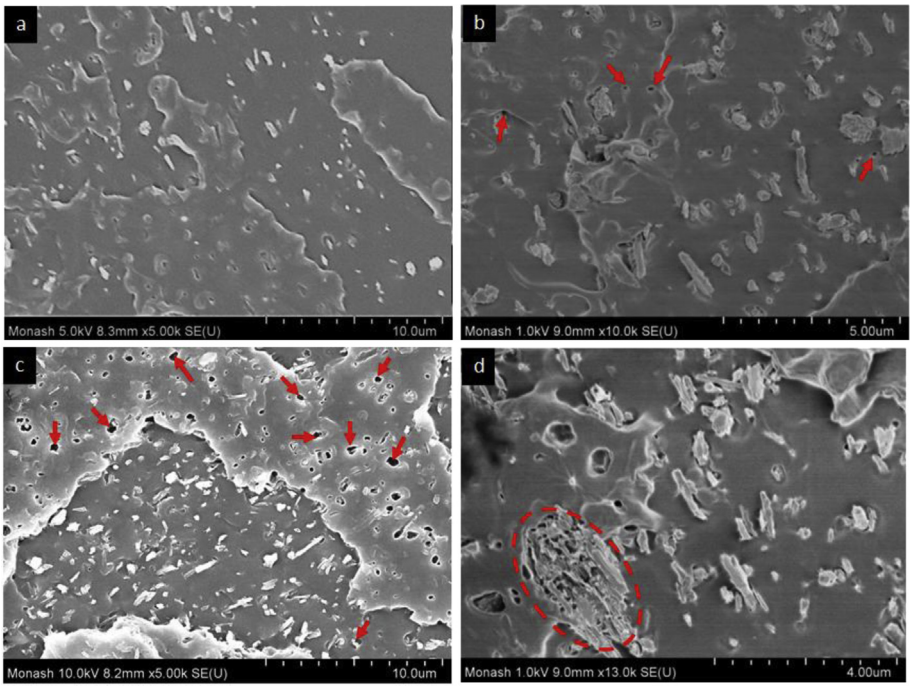

Fig. 8. Scanning electron micrographs of PLA nanocomposites with (a), (b) 5 (w/w %) and (c), (d) 10 (w/w %) of HNTs. Arrows show the "micro-voids" formation due to the pulled-out nanotubes. Circled part illustrates the aggregation of HNTs.

structure based model is more accurate compared to the idealized model and Halpin–Tsai analytical model for all concentrations of HNTs; for instance, elastic modulus of composites (E_c) predicted by real structure based model was 4.1% more accurate than the idealized model at 10 (w/w %) of HNTs. Furthermore, parametric studies were carried out to investigate the influence of the inclusion type (models with hollow tube-like and cylinder-like reinforcements) as well as the RVE size (amount of nanotubes), and it was found that the model with cylindrical reinforcements (representing HNTs) and at least 30 inclusions could efficiently predict the E_c of a polymeric nanocomposite reinforced by HNTs. Furthermore, stress and strain distributions of the FE models were analysed. This study demonstrated that the newly developed real structure based model can be successfully adopted to predict the E_c of HNTs based nanocomposites.

Acknowledgement

Financial support from FRGS/2/2013/TK04/MUSM/03/1 from the Ministry of Higher Education (MOHE), Malaysia, and technical and English grammatical comments and reviews given by Prof. Geoff Gibson (Newcastle University, UK) and Dr. Jock. G. Churchman (University of Adelaide) on this work is gratefully acknowledged. L.M. acknowledges the financial support of the Danish Council for Strategic Research (DSF) via the project "High reliability of large wind turbines via computational micromechanics" (Ref. no. 10-094539).

References

[1] Pasbakhsh P, Churchman GJ, Keeling JL. Appl Clay Sci 2013;74:47–57.
[2] De Silva RT, Pasbakhsh P, Goh KL, Chai S-P, Ismail H. Polym Test 2013;32(2):265–71.
[3] Hedicke-Höchstötter K, Lim GT, Altstädt V. Compos Sci Technol 2009;69(3–4):330–4.
[4] Deng S, Zhang J, Ye L. Compos Sci Technol 2009;69(14):2497–505.
[5] Mishnaevsky Jr L, Brøndsted P. Comput Mater Sci 2009;44(4):1351–9.
[6] Affdl JCH, Kardos JL. Polym Eng Sci 1976;16(5):344–52.
[7] Gómez-del Río T, Poza P, Rodríguez J, García-Gutiérrez MC, Hernández JJ, Ezquerra TA. Compos Sci Technol 2010;70(2):284–90.
[8] Prashantha K, Lecouvet B, Sclavons M, Lacrampe MF, Krawczak P. J Appl Polym Sci 2013;128(3):1895–903.
[9] Venkatesh GS, Deb A, Karmarkar A, Shivakumar ND. Prediction of the stiffness of nanoclay-polypropylene composites using a monte carlo finite element analysis approach. In: Chakraborty S, Bhattacharya G, editors. Proceedings of the international symposium on engineering under uncertainty: safety assessment and management (ISEUSAM – 2012). India: Springer; 2013. p. 1207–19.
[10] Peng RD, Zhou HW, Wang HW, Mishnaevsky Jr L. Comput Mater Sci 2012;60(0):19–31.
[11] Sheng N, Boyce MC, Parks DM, Rutledge GC, Abes JI, Cohen RE. Polymer 2004;45(2):487–506.
[12] Hbaieb K, Wang QX, Chia YHJ, Cotterell B. Polymer 2007;48(3):901–9.
[13] Dai G, Mishnaevsky Jr L. Compos Sci Technol 2014;91(0):71–81.
[14] Dai G, Mishnaevsky Jr L. Compos Sci Technol 2013;74(0):67–77.
[15] Wang HW, Zhou HW, Peng RD, Mishnaevsky L. Compos Sci Technol 2011;71(7):980–8.
[16] Lusti HR, Gusev AA. Model Simul Mater Sci Eng 2004;12:S107–19.
[17] Kari S, Berger H, Gabbert U. Comput Mater Sci 2007;39(1):198–204.
[18] Hine PJ, Rudolf Lusti H, Gusev AA. Compos Sci Technol 2002;62(10–11):1445–53.
[19] Lee WJ, Son JH, Kang NH, Park IM, Park YH. Scr Mater 2009;61(6):580–3.
[20] Sheidaei A, Baniassadi M, Banu M, Askeland P, Pahlavanpour M, Kuuttila N, et al. Compos Sci Technol 2013;80:47–54.
[21] Dong Y, Bhattacharyya D. Polymer 2010;51(3):816–24.
[22] Mortazavi B, Baniassadi M, Bardon J, Ahzi S. Compos B Eng 2013;45(1):1117–25.
[23] Liu H, Brinson LC. Compos Sci Technol 2008;68(6):1502–12.
[24] Lu D, Chen H, Wu J, Chan CM. J Nanosci Nanotechnol 2011;11(9):7789–93.
[25] Lecouvet B, Horion J, D'Haese C, Bailly C, Nysten B. Nanotechnology 2013;24. http://dx.doi.org/10.1088/0957–4484/1024/1010/105704.
[26] Mortazavi B, Hassouna F, Laachachi A, Rajabpour A, Ahzi S, Chapron D, et al. Thermochim Acta 2013;552(0):106–13.
[27] Wang HW, Zhou HW, Gui LL, Ji HW, Zhang XC. Compos B Eng 2014;56(0):733–9.
[28] Hua Y, Gu L. Compos B Eng 2013;45(1):1464–70.
[29] Chawla N, Sidhu R, Ganesh V. Acta Mater 2006;54(6):1541–8.
[30] Goh KL, Aspden RM, Hukins DWL. Compos Sci Technol 2004;64(9):1091–100.
[31] De Silva R, Pasbakhsh P, Goh K, Chai S-P, Chen J. J Compos Mater 2013. http://dx.doi.org/10.1177/0021998313513046.
[32] Liu M, Zhang Y, Zhou C. Appl Clay Sci 2013;75-76:52–9.